ANALYSIS OF A THERMAL BRIDGE IN A GUARDED HOT BOX TESTING FACILITY

K. Martin[a], A. Campos[b], C. Escudero[a], I. Gómez[b], J.M. Sala[b]

[a]Laboratory for the Quality Control in Buildings - Basque Government
C/ Agirrelanda n. 10, 01013 Vitoria-Gasteiz, Spain
[b]Department of Thermal Engineering – University of the Basque Country (UPV/EHU), Alameda Urquijo s/n. 48013 Bilbao, Spain

E-mail: koldobika.martin@ehu.es
Tel.: + (34) 94 601 7378, Fax: + (34) 94 601 4283

ABSTRACT

Nowadays, several regulations exist covering different general guidelines that must be considered in order to decrease the energy demand in residential buildings. One of the main ones consists in increasing the insulation of the building envelope with the aim of minimizing heat losses or gains. As a result, a proper treatment of thermal bridges and their in-situ construction becomes more relevant because their relative effect on the overall thermal demand of the building increases.

Nevertheless, there is still a great uncertainty about the dynamic behavior of thermal bridges and few energy simulation programs allow implementing them considering their thermal inertia.

To obtain more information about the thermal response of thermal bridges, a series of tests have been carried out in a guarded hot box testing facility. The characteristics of a pillar thermal bridge have been studied in both steady and dynamic regime, being one of the main objectives of this study the determination of the area of influence of a thermal bridge. For this purpose, test results are compared with simulation ones.

KEYWORDS: Thermal bridge, testing, guarded hot box, simulation, dynamic regime, thermal inertia.

1. Introduction

Today one of the outstanding tasks in achieving an efficient thermal performance in buildings is the correct modeling of thermal bridges (TBs) in energy demand programs. It has already been demonstrated the great importance of TBs when the thickness of the insulation layer is increased [1]. Theodosiu in [2] asserts that TBs can signify 30% of the final demand.

However, the method used to calculate the effect of thermal bridging must be taken into account when analyzing this result, since the percentage can vary up to 11% [3]. The models employed to characterize TBs in building simulation programs generally do not take into account their inherent inertia and are based on the linear thermal transmittance (Ψ) which is the heat flow rate in the *steady state* divided by length and by the temperature difference between the environments on either side of a TB [4] and it is calculated according to Eq. (1). Another feature to consider is that the real influence of a particular TB is unknown, namely the surface of the envelope actually affected by the TB.

$$\Psi = L_{2D} - \sum_{j=1}^{N} U_j \cdot l_j \qquad (1)$$

where,

L_{2D} is the thermal coupling coefficient obtained from a 2D calculation of the component separating the two environments being considered [W/mK].
U_j is the thermal transmittance of the 1D component, j, separating the two environments being considered [W/m^{2}K].
l_j is the length over which the value U_j applies [m].

Programs seeking to implement the effect of TBs on entire buildings usually make a number of simplifications that often lead to assigning the thermal inertia of the surrounding homogeneous wall to the TB itself [5,6]. This leads to big mistakes in those constructive solutions whose inertia differs from the homogeneous wall such as in the window contour TBs case. Owing to the different thermal behaviors achieved by applying different calculation models to the same TB [7], it arises the necessity of knowing the real answer to a given excitation, and then to extrapolate these results to the real weather conditions.

Although it would be appropriate to make in situ measurements [8], such monitoring procedure involves a too big uncertainty caused by a large number of factors such us closeness between different thermal bridges, difficulty in finding homogeneous areas, devices that can alter the measurements, user habits, need of a nearby weather station, etc.

To perform simple and controlled measurements, a guarded hot box unit is employed wherein the quality of the results depends only on the accuracy of the sensors used and on the performance of the environmental chambers [9]. The construction of the samples is made under the supervision of the technical staff at the Construction

Quality Control Laboratory (LCCE) of the Basque Government. This avoids the uncertainty of not knowing exactly the constructive solution where measurements are made and facilitates data for subsequent simulations.

2. Guarded hot box testing facility

The LCCE in Vitoria-Gasteiz has available an equipment (Fig.1) for the measurement of the thermal resistance (R_t) of opaque walls designed and calibrated according to the standard EN ISO 8990 [10] The apparatus comprises mainly two air-conditioning chambers, the *hot chamber* and the *cold chamber*, where the inside and outside conditions of the dwelling respectively are simulated. The two chambers have an indirect system of thermoregulation with a rate of 0.2 K/min and an accuracy of ± 0.2 K. The testing sample is placed between both chambers (Fig. 2).

Around the lateral side if the sample there is a third chamber called *tempering ring*, in charge of minimizing the heat flux through the perimeter of the sample. Inside the hot chamber there is a fourth chamber being composed of a 8 cm thick sandwiched panel , referred to as *metering box* (1 x 1 x 0.5 m). The mouth of the metering box (1.065 m^2) is set in contact with the sample at the same temperature as the surrounding chamber. Since no temperature difference exists between both environments all the heat generated inside the box (resistances and fans) leaks exclusively through the sample.

Inside each of the chambers there is a group of 86 type T thermocouples, which measure the temperature of the air and the sample surface, both in the measuring and in the guarded zone.

During the test there are different parameters to be controlled in order to get temperatures throughout the sample as uniform as possible. Such parameters are the temperatures in the cold and hot chamber, in the metering box and in the tempering ring (which is set at a mean temperature between the hot and cold chambers) and the air velocities within the hot and cold chambers as well.

The error estimation of the test procedure was 2,3% in the last verification test carried out with an homogeneous well known sample (XPS 5 cm) according to ISO 8990.

When the goal is to characterise the dynamic behaviour of a sample, the testing method used for the measurement of the thermal transmittance has to be modified. This is due to the fact that the metering box is not able to regulate in the same way as the surrounding chamber, because it is not provided with cold equipment, and therefore this would yield two zones with different temperatures.

The alternative method consists in disconnecting and removing the metering box from the wall surface and performing the heat flux measurement with two 0.5 x 0.5 m flux meters placed in the central region of both sample sides. The use of flux meters entails a number of disadvantages with respect to the hot-box method which yields a worse accuracy in the flux measured.

3. Test methodology

3.1. Description of the samples

As said before, linear thermal transmittance (Ψ) can be defined as the added heat flux through a TB respect to the same solution without the TB per meter of length and when a temperature difference of 1 C is applied between both sides. Thus, in order to obtain this parameter, both the wall with the TB and the homogeneous wall must be thermally characterized. For this reason two different samples are built up

These samples are built within an Iroko wood frame with a 0.17 m thickness and internal dimensions of 2 x 2 m (Fig. 3). The heat flux is measured through a 1.065 m^2 metering area, belonging the rest of the surface to the guarded zone.

The difficulties involved in TBs testing are mainly due to the geometric construction and also to the multidimensional character of the heat flux that a TB entails [11]. To overcome these problems, the geometry of one of the few TBs that can be tested in the hot box unit has been adapted. The homogeneous wall design is based on the type of F3.22 façade (Fig. 4) according to the Spanish Catalogue of Building Elements (CBE) [12].

The homogeneous wall differs only in two details from the solution shown in Fig. 4. The thickness of the air gap is reduced to 0.025 m and on the other hand, the block used to build up the inner sheet has a 0.06 m thickness, being 0.04 m the thickness of the insulation layer.

The pillar inside the wall has been the chosen TB to carry out the tests and it is based on the Pi2.1.3 type of the CBE (Fig. 5). This corresponds to a pillar coated on the outer surface and backfilled with insulation and a brick factory. According to the CBE with this type of TB surface condensation will not occur in any Spanish climate zone.

Due to the geometrical constraints imposed by the guarded hot box facility, the choice of the TB from Fig. 5 is the solution which best fits to this kind of tests. Nevertheless, the configuration of Fig. 5 has necessarily to be modified to facilitate the work of testing, specifically

the placement of heat flux meters and thermocouples. This modification consists on leaving the inner surface of the sample at the same plane. With this purpose, the reinforced concrete pillar is reduced to 0.22 x 0.22 m. The sketches of the tested samples are defined in Fig. 6 while the thermal properties of the used materials appear in Table 1.

The thermal properties listed in Table 1 were obtained from different sources. The thermal conductivity of the plaster and the insulation were obtained from tests on a guarded hot plate facility [13] while the equivalent thermal conductivity of the masonry products were derived from simulations validated with tests in a hot box facility. All the densities (except for the air) were calculated measuring the weight of each material. Finally, for materials for which no information was available by these means, values from the material properties database within LIDER have been used. LIDER is the Spanish official software which establishes a limit to the energy demand in residential buildings [14].

In literature [15] lower values of specific heat can be derived for mortar and concrete. Thermal inertia of the sample is influenced by the specific heat, density and thermal conductivity. It must be taken into consideration that lower values of specific heat mean lower inertia, and thus higher amplitude and smaller phase lag in the dynamic response.

A TB with a bigger effect could have been designed, for example without insulation in the pillar zone, but one of the goals of this research is to focus on the characterization of TBs that comply with the current Spanish legislation. In this case the insulation thickness surrounding the pillar is half the one corresponding to the homogeneous wall.

To avoid uncertainties in the results due to the effect of moisture on the thermal properties of materials, samples are conditioned in an environment at 296 K and 50% relative humidity till they achieve weight stability. Once the weight variation of the sample among the last two weighing is less than 1% [10] the sample is supposed conditioned and then the test can be carried out.

3.2. Test in steady regimen

The test in steady state consists in fixing a temperature difference between both sides of the sample in order to define the thermal resistance value (R_t) or, analogously, its corresponding transmittance (U). For such purpose, the air temperature of the cold chamber is set to 0°C and the temperature of the hot chamber and of the metering box is set to 20°C. Under these conditions the power generated inside

the hot box matches up with the heat flux passing through the sample. By measuring the power generated and the temperature difference between the hot and cold surfaces, the thermal resistance of the sample is obtained.

$$R_t = \frac{T_{si} - T_{so}}{\Phi / A} = \frac{\Delta T}{\Phi / A} \qquad (2)$$

being,

T_{si}, T_{so} the inner (hot side) and outer (cold side) surface temperature in [K].
Φ the power generated within the hot box in [W].
A the area of the measuring surface in [m^2].

The thermal resistance (R_t) is expressed in m^2K/W. On the other hand the thermal transmittance (U) is the parameter usually used to limit energy demand through the building envelope, defined as follows:

$$U = \frac{1}{R_T} = \frac{1}{R_{si} + R_t + R_{so}} \qquad (3)$$

being,

R_{si}, R_{so} the inner and outer surface resistances in [m^2K/W]
R_t the surface to surface thermal resistance in [m^2K/W]
R_T the air to air thermal resistance in [m^2K/W]

Usually, in laboratory tests the R_t value is measured and then, in order to obtain the U values, the standardized surface resistance values according to EN ISO 6946 (R_{si} and R_{so}) [16] are added. In the case of horizontal heat flux the standard provides R_{si}=0.13 m^2K/W and R_{so}=0.04 m^2K/W.

3.3. Test in dynamic regimen

Nowadays there are no regulations regarding testing in dynamic conditions, so in this section the methodology carried out will be briefly explained [17]. The main difference between the tests performed in steady and dynamic regimen is that in the latter, it is necessary to use heat flux meters instead of the guarded hot box. This represents a loss of accuracy in the measurements. Furthermore, the use of heat flux meters presents another series of disadvantages:

- The measuring zone is smaller (0.24 m^2 or 0.032 m^2 depending on the heat flux meter versus 1.065 m^2 in the hot box), which may not be representative enough of the testing sample.
- The contact with the sample in the flux meters is not perfect, thus a little air chamber may remain between the flux meter and the measuring zone. In order to minimise this measurement error, a conducting paste can be applied between the flux meter and the measuring zone.
- The air currents that uniform the temperatures in the climatic chambers and which vary according to the regulation of their temperature and velocity setpoints have an influence on the output signal of the heat flux meters.
- In case of the measurement of small heat fluxes, due to the low sensitivity of the heat flux meters, the signal provided results too distorted and not suitable for the calculations. Therefore the data from the heat flux meter must be treated in order to obtain a curve which fits with the measured data.

Information about the employed heat flux meters produced by Ahlborn is shown in Table 2. They are stuck to the surface of the wall with a thin conductive paste. To ensure a proper functioning of the heat flux meters and so to reduce the error of measurement, a series of preliminary tests are necessary to be carried out:

1. Before starting any dynamic analysis, the constructive solution must already have been characterized in steady state. This test is carried out according to the EN ISO 8990 standard, applying a ΔT =20 K between both sides of the wall ($T_{Hot\ Chamber}$ = 293 K and T= 273 K) and using the metering box to obtain the R_t of the wall.

   This test allows determining the exact setpoints for the temperatures and the speed that it will be used in the following tests. Apart from the setpoints, the average value of the power delivered by the box is used as a parameter for the calibration of the heat flux meters.

2. The following test consists on repeating the previous one but this time removing the metering box from the wall, which means that only heat flux meters are used for measuring the heat flux. In this manner the proper functioning of the heat flux meters with the previously calculated calibration parameters can be verified. Having the mean values of air temperature on both sides and with the heat flux meters calibrated, the mean value of the surface resistances can be obtained.

3. In the last test the temperatures of the two chambers are fixed at 293 K. The main goal is to know the offset that may have the flux meters. As the temperature gradient between the two sides of the wall is null, the heat flux must also be null. So the signal that

the heat flux meters measures during this test is regarded as the offset.

The metering box is an element that varies the air stream that runs along the wall surface in the hot chamber. As the dynamic tests are performed without the box, the conditions for the measurement of the film coefficients have to been reproduced as accurately as possible for the later use in the simulation. Thus when the test reaches the stability, the calculation of surface resistances is performed as follows:

$$\begin{cases} R_{so} = \dfrac{|T_{so} - T_o|}{\Phi / A} \\ R_{si} = \dfrac{|T_{si} - T_i|}{\Phi / A} \end{cases} \qquad (4)$$

Once the steady tests are finished, the dynamic test can be made, which involves applying a sinusoidal excitation according to Eq. (5) in the cold chamber, while the hot chamber is kept at a constant temperature of 293 K. The way the heat flux wave passes through the homogeneous wall will be analyzed. Afterwards, these results will be compared to those obtained from the sample with the TB.

$$T_o = 293 + 10 \cdot Sin\left(\frac{\pi}{12} \cdot t - 3\right) \qquad (5)$$

The main parameters to be obtained for later comparison are the thermal amplitude and the phase lag of the heat flux. The latter is defined as the time between the minimum temperature in the cold chamber and the maximum value of the heat flux in the hot chamber. To decouple the influence of the inertia on the thermal response of the sample, the sinusoidal excitation is repeated five times being of interest just the last cycle.

4. Definition of the simulation

In addition to analyzing the results from the tests in the guarded hot box facility, simulations of the same constructive solutions are carried out. The purpose of this simulation is to analyze both the differences between test results and numerical calculation and also to get the capability to extrapolate results to other types of thermal bridges, as in the simulation there are not the geometric constraints that have been found in the test facility.

To make a correct comparison, the boundary conditions used in the simulation are taken from values measured in tests. The scheme of the dynamic simulation is defined in Fig. 7.

The numerical simulations are performed through the finite volume simulation tool FLUENT 6.2 [18], which solves the simplified equation of energy, Eq. (6), for each time step and node defined by the mesh. The mesh is constructed using the pre-processor GAMBIT 2.2. The simplicity of the geometries allows using a mesh consisting of 5 mm size rectangular and structured elements (Fig. 8), not exceeding in any case the 27,000 elements, and thus achieving an optimal mesh quality.

$$\frac{\partial}{\partial t}(\rho \cdot h) = \nabla(\lambda \nabla T) \qquad (6)$$

being,

ρ the density [kg/m^3]

h the enthalpy [J/kgK]

λ the thermal conductivity [W/mK]

T the temperature [K]

To decouple the transient effects, the simulation is performed for 3 days using a time step of 200 s and employing for later calculations results only from the last day.

5. Results

5.1. Sample without thermal bridge

5.1.1. *Test in steady state*

The first test is conducted according to EN ISO 8990 and therefore is carried out working with the metering box. To obtain the R_t value, which characterizes the sample in steady state, is the main objective. This value is dependent on the power generated by the metering box and on the surface to surface temperature difference. The surface temperature is taken from the average value of the thermocouples of the metering zone and the power is calculated by integrating the energy generated over the test since the heat flux has become steady.

$$R_{test} = \frac{(T_{si} - T_{so}) \cdot A}{\Phi} = \frac{(19.36 - 0.76) \cdot 1{,}065}{10.48} = 1.890\ \mathrm{m^2 K/W}$$

This test complies with the limits set out in the Annex A of EN ISO 1946-4 [19] about the characteristics of the equipment and test conditions. Under these conditions an uncertainty of 5% in the R_t value is estimated.

The result of the thermal resistance from the test can be compared with the resistance numerically calculated, R_{calc} = 1,909 m^2K/W, using the thermal properties of the materials defined in Table 1. As we can appreciate the results are very close. Each method has its own sources of error, so in this case we cannot assert which method is more accurate. To evaluate the relative error committed between these two procedures, Eq.(7) is used [20]:

$$e_{1-2} = \frac{|R_1 - R_2|}{\overline{R}} \cdot 100 \qquad (7)$$

being,

$\overline{R}$ the average value of thermal resistance calculated using the methods compared [m^2K/W].

According to Eq. (7) the error in the calculation of the thermal resistance is $e_{test-calc}$ = 0.99%. It can be seen that errors in the results between the two methods are even lower than the uncertainty of each method separately.

5.1.2. Dynamic test

As there is no standardized procedure for tests in transient regime as well as for the characterization of TBs, it is necessary to design a new one. As in TBs there are different thermal zones, there is a need to define a new strategy for the placement of the sensors. This strategy is based on the same basis as in the EN ISO 8990, namely defining a metering zone and a guarded zone. In order to be able to analyze the area of influence of the TB now we will have to consider two areas of measurement per side, with their corresponding guarded areas. In the central zone we will measure higher heat fluxes because of the influence of the pillar whereas the locations of the thermocouples are fixed in the surrounding of the heat flux meters (Fig. 9).

There are four heat flux meters, two large ones with a meander size of 0.49 x 0.49 m (I in the non-excited surface and II in the excited surface) and two small ones with a size of 0.18 x 0.18 m (III in the non-excited surface and IV in the excited surface). The large ones are situated in the central zone and the small ones placed in a side facing each other. The aim of this placement is to collect data on the TB area and in an area as far as possible from the TB (within the space limitations of the facility.)

According to the configuration of the thermocouples in Fig. 9b, 4 thermocouples are used for each measurement area. The average value is used in the calculations.

The sample without TB, composed of homogeneous layers, does not need the collection of data from different areas because the heat flux is basically one-dimensional. Even then, for a better comparison with the sample containing the TB, it is also considered the configuration depicted in Fig. 9b.

Once the test is finished, the following step is to obtain the equations which define the fitting curves. By applying a sinusoidal excitation in the cold chamber, the other parameters to be analyzed will also be defined by a sine function according to the equation Eq. (8) and the coefficients listed in Table 3.

$$y = y_0 + A \cdot Sin\left(\frac{t - x_c}{w}\pi\right) \qquad (8)$$

The constants of the fitting curves show that, in the hot chamber, slightly higher temperatures are reached in the side when compared with the central zone (ΔT = 0.2 K), while in the cold chamber the opposite effect occurs (ΔT = 0.1 K). It can be assumed that these differences are low enough since they are within the measurement uncertainty range of the thermocouples. The fitting curves conform well to the heat flux meters signal (Fig. 11 and Fig. 12) and the R^2 error term refers more to the dispersion experienced by the signal with respect to the fitting curve than the error made in the fitting.

Having defined the fitting curves, the comparison between the heat fluxes obtained from the test and from the numerical calculation is straightforward (Fig. 13).

As the probe is a homogeneous layers wall, the heat flux reaching in the central and side zones of each chamber practically is the same. Despite the uncertainties associated to the test and to the numerical calculation, Fig. 13 shows the similarity between the responses to sinusoidal excitation. This similarity is shown in more detail in Table 4 which describes the values of the amplitude and phase lag for the heat flux in the non-excited surface.

Although without knowing which method of calculation is closest to reality, we should take into account that slightly lower heat flux values are obtained in the simulations.

5.2. Sample with thermal bridge

5.2.1. *Test in steady state*

The standard EN ISO 8990 is not going to be applied to samples with TBs by the following reasons. The fact that the heat flux in these samples is multidimensional does not ensure many of the

specifications imposed by the standard. Furthermore, the dimensions of the metering box do not cover the distance from the TB to the cut-off plane proposed by the standard ISO 10211 [21] in its method of calculation.

Nevertheless, the test in steady state has been carried out, although it is important to consider its limitations:

- There is a heat flux parallel to the sample (Fig. 14) which produces a heat flux imbalance.
- The temperature distributions on the surfaces of the sample are non-uniform.
- The metering area may not be representative of the test sample.

The heat flux imbalance occurs when the heat finds a "preferential way" to pass through the sample. Fig. 14 shows isotherms by applying a jump of 20°C. As the heat flux is perpendicular to isotherms, an extra heat flux not generated by the metering box enters the central area. This makes the measured power generated by the hot box being lower than the one the sample really needs to reach the steady state, achieving a greater R_t value.

$$R_t = \frac{(T_{si} - T_{so}) \cdot A}{\Phi} = \frac{(19.29 - 0.83) \cdot 1.065}{12.24} = 1.606\,\mathrm{m}^2 K/W$$

The value obtained by the hot-box test facility can be compared with calculations based on different models. Performing simulations corresponding to the same dimensions of the test sample (width = 2 m), one gets R_t = 1.610 m^2K/W. Simulating only the area occupied by the box (width = 1 m), the resistance is R_t= 1.405 m^2K/W. Comparing the latter value with that obtained from test data it is shown the effect of parallel flux by increasing the R_t value. Finally it has also been simulated under the same thermal specifications of ISO 10211, where the cut-off planes should be located at least 1 m from the flanking element (width = 2.26 m), obtaining a R_t = 1.638 m^2K/W.

It should be noted that the bigger the width of the homogeneous zone, the greater is its proportion with respect to the TB and therefore, the overall thermal resistance of the constructive solution becomes greater.

Multiple cut-off planes are discussed because in future papers an equivalent wall method will be analyzed which to implements TBs in a BES (Building Energy Simulation) program. That is why there is the need of a method in which the dimensions of the constructive

element are fixed in order to characterize the TB and then to transfer to the geometry of the building to be simulated.

A similar phenomenon was observed when analyzing the average values of the heat flux meters. I and II heat flux meters measure approximately the same heat transfer through the pillar area, 17.94 W/m^2 and 18.42 W/m^2 respectively. These values can be compared with those measured in the hot box, 12.24 W/m^2. The conclusion is the same obtained above from the simulation, the bigger the measurement area is the lower the heat flux density. The heat flux meters occupy the width of the pillar plus 27 cm of homogeneous wall, while the hot box occupies the pillar box plus 0.78 m of wall.

5.2.2. *Dynamic test*

The aim of this last test is to analyze the heat flows in the zone of the pillar and away from it and then to compare these test results with those achieved from the homogeneous wall. To do this, once again fitting curves are used.

The conclusions that can be derived from Table 5 are similar to those from Table 3. After data processing of the test results, simulations are carried out considering 2 meters of width (like the tested sample).

When analyzing the results of the wall with TB, it should be highlighted that the heat flux obtained from the simulation corresponds to a width of 2 m, while the heat flux from the sensors is for a width of 0.49 m or 0.18 m. Therefore in the simulation the influence of the homogeneous part is bigger and thus the expected heat flux density is lower.

Similar inertia is found for the right picture in the Fig. 15, when comparing the pillar zone and the homogeneous part. It can also be noted that there are more losses (or gains) in the area of the pillar. The results from the simulation are presented in Table 6.

5.3. Calculation of linear thermal transmittance

Once the limitations offered by the guarded hot-box test for heterogeneous solutions are known, the linear thermal transmittance (Ψ) of the TB is calculated. The standard ISO 10211 defines the boundary conditions that have to be considered in a constructive solution for the calculation of Ψ. Nevertheless, in the test there are several possibilities and criteria for the calculation of Ψ depending on the device employed for the measurement of the heat flux.

The calculation is performed varying both the geometrical dimensions and the boundary conditions depending on the requirements of the

model. The aim is to study the variability of Ψ according to the different models under consideration.

The "l" value depicted in Fig. 16 refers to the area of heat flux measurement for each test case. The length of the flanking element is taken from the point where the homogeneous wall varies (0.26 m).

The thermal coupling coefficient (L^{2D}) is the heat flux obtained by the tested or simulated procedure when applying a temperature difference of 1 K. The variation of the surface resistances R_{si} and R_{so} does not imply major changes in the calculations, since for the calculation of the thermal transmittance it is the value of their sum what matters and this value does not introduce big changes.

In spite of using different geometries for the calculation of L_{2D}, the variations observed in Ψ values were very low. Taking the method of the ISO 10211 as the reference, a greater accuracy is observed with the simulation in comparison with the tests. This is due to the aforementioned problem of parallel heat flow.

The difference between the results of the simulations when taking l = 2.26 m or l = 0.49 m is quite low. This means that different models present the same stationary behavior, but different dynamics. This effect is intended to be implemented in simulation of buildings.

5.4. Comparison between the two samples

So far, the test results have been compared with the results of simulations for each type of wall. In this section, the test results are directly compared in order to examine the differences between a wall of homogeneous layers and the wall with the pillar embedded in the facade. The study focuses on the heat flux in the non-excited surface, which is what matters in assessing the energy demand of buildings.

The influence the pillar has on the heat fluxes and temperatures is obvious. It is not so clear and of great interest to know to which extent the lateral side of the sample with TB is altered by the presence of the pillar.

A priori, the greatest differences in amplitude of the heat flux and phase lag appear in the central area of the walls (Fig. 17). As it has been stated before, the inertia of the pillar and the homogeneous wall is similar, so for this particular TB, no great disparities in the phase lag are going to be found. In the central zone the heat flux wave through the wall appears with a greater magnitude in the pillar area and just 26 min earlier. The so analyzed TB is partially corrected with a 0.02 m insulation layer, but in [7] it is demonstrated that differences in other configurations of TBs could be greater.

In contrast to the central area, i n the lateral area of the samples the amplitude of the internal heat flux is slightly higher in the wall without TB, giving rise to a very small phase lag ($\Delta\varphi$ = 4 min). All this appears summarized in Table 8:

6. Conclusions

With the aim of analyzing the real behavior of TBs, a series of tests in steady and dynamic state have been carried out in a guarded hot box facility. To this end two similar samples have been built in the LCCE, one containing the pillar TB and the other without it.

The test conducted in accordance with the standard EN ISO 8990 for the homogeneous wall agrees very fairly with the numerical calculation carried out with FLUENT software, with an error lower than 2%. This error is under the uncertainties of each method.

A different situation is found when analyzing the wall that contains the TB. This is due to the limitations that present the guarded hot box test for the characterization of heterogeneous samples. On the one hand, there is a multidimensional flux which distorts the test results. On the other hand, the fact that the metering box (or the heat flux meters) can not cover a sufficiently representative area of the TB. Still the R_t value does not vary by more than 8% with respect to the value obtained by calculation according to ISO 10211.

Another remark reached from this study is that the R_t and Ψ thermal parameters vary depending on the measurement area of the sensor and the length of the simulated constructive solution. In the calculation of Ψ the biggest errors are achieved when using test data compared with the results of the standardized method. Notably, with lengths shorter than those set out in the ISO 10211, good results for Ψ are achieved. The fact that the stationary parameters change according to these geometric characteristics suggests that the dynamic characteristics also vary.

A methodology to deal adequately with the least possible uncertainty is developed for the dynamic testing. In this procedure factors such as sample humidity, surface resistances, calibration of heat flux meters and inertia of the wall are controlled, running an overall of three stationary tests before the dynamic one could be started.

The dynamic tests, in which one surface is excited with a sine wave, are mainly used in order to obtain values of the amplitude and the phase lag of the internal heat flux, with the aim of comparing easily results of tests and simulations. In the sample without TB, the results are very similar to those the theory states, namely there are similar

heat fluxes in whatever area of the surface. However the results from the simulation are found to be slightly lower.

On the sample containing the pillar, due to the inertia equality between the central area and lateral side, the largest differences occur in the amplitudes of the fluxes, being these amplitudes greatest in the central area. In the simulation, heat flows on the non excited surface almost overlap with those of the lateral area in the test. This raises definitely the idea that the geometric conditions defined by the ISO 10211 are not suitable for dynamic system characterization. According to the test results, the influence that TB has on the simulated heat flux should be higher per unit area. Logic says that the response of the TB should be between the data of the heat flux meter I and III.

In future papers a methodology to choose the influence zone of any TB will be presented. In this way using thermoelectric analogy, a wall consisting of three homogeneous layers behaving like the TB can be calculated. Linking the influence area to this equivalent wall, TBs can be implemented in building simulation programs taking into account not only the loss of heat added by TBs, but also their inherent inertia.

References

[1] G. Mao. Thermal Bridges. Efficient Models for Energy Analysis in Buildings. Department of Building Sciences, Kunglika Tekniska Högskolan, Stockholm (1997).

[2] T.G. Theodosiou, A.M. Papadopoulos. The impact of thermal bridges on the energy demand of buildings with double brick wall constructions. Energy and Buildings, 40, 2083-2089 (2008).

[3] M. Spiekman. Contribution to the ASIEPI project: Summary of a Dutch study on the quantification of thermal bridge effects on the energy performance. Summary report of ASIEPI WP4 (available to the end of the project).

[4] A. Ben Larbi. Statistical modelling of heat transfer for thermal bridges of buildings. Energy and Buildings, 37, 945-951 (2005).

[5] J. Sala, M. Machatka. Common thermal defects and failures of prefabricated buildings and their rehabilitation. KEA, Technology Centre AS CR, Prague (2002).

[6] A. Campos, K. Martín, C. Mvuama, C. Garcia, M. Odriozola, J.M. Sala. The effect of thermal bridges on the thermal comfort of buildings. 4th International Building Physics Conference, Istanbul, Turkey (2009).

[7] K. Martin, A. Erkoreka, I. Flores, M. Odriozola, J.M. Sala. Problems in the calculation of thermal bridges in dynamic conditions. Energy and Buildings, 43, 529-535 (2011).

[8] M. Cucumo, A. De Rosa, V. Ferraro, D. Kaliakatsos, V. Marinelli. A method for the experimental evaluation in situ of the wall conductance. Energy and Buildings, 38, 238-244 (2006).

[9] W.C. Brown and D.G. Stephenson. A guarded hot box procedure for determining the dynamic response of full-scale wall specimens. Part I. ASHRAE Transactions, 99, 632-642 (1993).

[10] EN ISO 8990: Thermal insulation. Determination of steady-state thermal transmission properties. Calibrated and guarded hot box (1996).

[11] G. Mao. Laboratory measurements and modeling of the dynamic thermal performance of residential wall systems. Nordic Journal of Building Physics, 1 (1997).

[12] Eduardo Torroja Institute in collaboration with CEPCO and AICIA. Catálogo de elementos constructivos. Building Ministry, Government of Spain (2008).

[13] EN 12667: Thermal performance of building materials and products, Determination of thermal resistance by means of guarded hot plate and heat flux meter methods, Products of high and medium thermal resistance (2001).

[14] LIDER, Ministry of Housing, 2007

[15] R. Cerny, J. Toma and J. Sestak. Measuring the effective specific heat of building materials. Thermochimica Acta, vol. 282-283, 239-250 (1996).

[16] EN ISO 6946: Building components and building elements. Thermal resistance and thermal transmittance. Calculation method (1996).

[17] K. Martin, I. Flores, C. Escudero, A. Apaolaza, J.M. Sala. Methodology for the calculation of response factors through experimental tests and validation with simulation. Energy and Buildings, 42, 461-467 (2010).

[18] FLUENT 6.2. User's manual, ANSYS Inc. (2005)

[19] EN ISO 1946-4: Thermal performance of building products and components. Specific criteria for the assessment of laboratories measuring heat transfer properties. Part 4: Measurements by hot box methods (2000).

[20] J. Kosny and E. Kossecka. Multi-dimensional heat transfer through complex building envelope assemblies in hourly energy simulation programs. Energy and Buildings, 34, 445-454 (2002).

[21] ISO 10211: Thermal bridges in building construction. Heat flows and surface temperatures. Detailed calculations (2007).

TABLES CAPTION

	Material	d [m]	λ [W/m·K]	ρ [kg/m^3]	c [J/kgK]
1	Plaster	0.015	0.28	1166	900
2	Perforated brick	0.06	0.40	921	1077
3	XPS rigid foam	0.04 - 0.02	0.034	29	800
4	Air cavity	0.025	0.15	1	1006
5	Lightweigth clay ceramic block	0.14	0.41	969	1077
6	Mortar	0.015	1.00	1700	1000
7	Reinforced concrete	0,22$^{(1)}$	2.30	2400	1000

Table 1 - Thermal properties of the constructive solutions

(1) Thickness of the rectangular pillar.

Type	Dimensions [mm]	Meander size [mm]	Substrate	Temperature Stability	Accuracy of Calib. Value
119	250x250x1.5	180x180	epoxy resin	80 ºC	5% at 25 ºC
150-2	500x500x0.6	490x490	teflon	150 ºC	5% at 25 ºC

Table 2 – Information about the heat flux meters

	Hot Chamber (Indoor)				Cold Chamber (Outdoor)			
	T_{wall_I}	T_{wall_III}	q_I	q_{III}	T_{wall_II}	T_{wall_IV}	q_{II}	q_{IV}
x_c	18.8	18.9	8.64	8.61	12.5	12.5	9.30	9.30
w	12.1	12.0	11.98	12.00	12.0	12.0	12.02	12.01
A	0.1	0.1	1.90	1.84	7.5	7.3	55.53	57.29
y_0	20.0	20.2	-0.14	0.12	19.9	19.8	0.31	0.08
R^2	0.83	0.92	0.79	0.88	1.00	1.00	1.00	1.00

Table 3 - Values of the coefficients for the fitting curves and the R^2 coefficient for the homogeneous wall

Method	A_{q_int} [W/m^2]	φ [h]
I fitted	1.91	8.1
III fitted	1.84	8.1
Simulation	1.59	7.9

Table 4 - Amplitudes and phase lags of the heat fluxes in the non excited surface

	Hot Chamber (Indoor)				Cold Chamber (Outdoor)			
	T_{wall_I}	T_{wall_III}	q_I	q_{III}	T_{wall_II}	T_{wall_IV}	q_{II}	q_{IV}
x_c	20.1	-4.0	8.71	8.96	13.1	13.0	10.68	9.75
w	12.1	12.0	12.05	12.04	12.0	12.0	12.00	12.02
A	0.1	0.1	2.54	1.62	6.2	7.3	65.89	66.36
y_0	20.0	20.1	-0.04	0.14	19.9	19.8	1.25	0.52
R^2	0.85	0.67	0.76	0.77	1.00	1.00	1.00	1.00

Table 5 - Values of the constants of the fitting curves and R^2 coefficient for the simple with TB

Method	A_{q_int} [W/m^2]	φ [h]
I fitted	2.53	7.7
III fitted	1.61	8.0
Simulation	1.64	8.1

Table 6 - Amplitude and phase lag of the heat flux in the sample with TB

nº	Method	R_{si} [m^2K/W]	R_{so} [m^2K/W]	l [m]	L^{2D} [W/mK]	ΔT [K]	Ψ [W/mK]	Error [%]
1	Test: Methering box	0.063	0.080	1.00	0.61	20.2	0.11	36.5
2	Test: Central heat flux meter	0.063	0.080	0.49	0.44	20.2	0.20	11.1
3	Simulation: Model 1	0.063	0.080	1.00	0.65	20.0	0.17	7.8
4	Simulation: Model 2	0.063	0.080	0.49	0.43	20.0	0.19	4.5
5	Simulation: ISO 10211	0.130	0.040	2.26	1.27	20.0	0.18	0.0

Table 7 - Comparison of models in the calculation of Ψ

	Heat Flux Meter I		Heat Flux Meter III	
	A_{q_int} [W/m^2]	φ [h]	A_{q_int} [W/m^2]	φ [h]
Without TB	1.91	8.1	1.84	8.1
With TB	2.53	7.7	1.61	8.0

Table 8 – Amplitude and phase lag of the interior heat flux in the central zone

FIGURES CAPTION

Figure1

Figure2

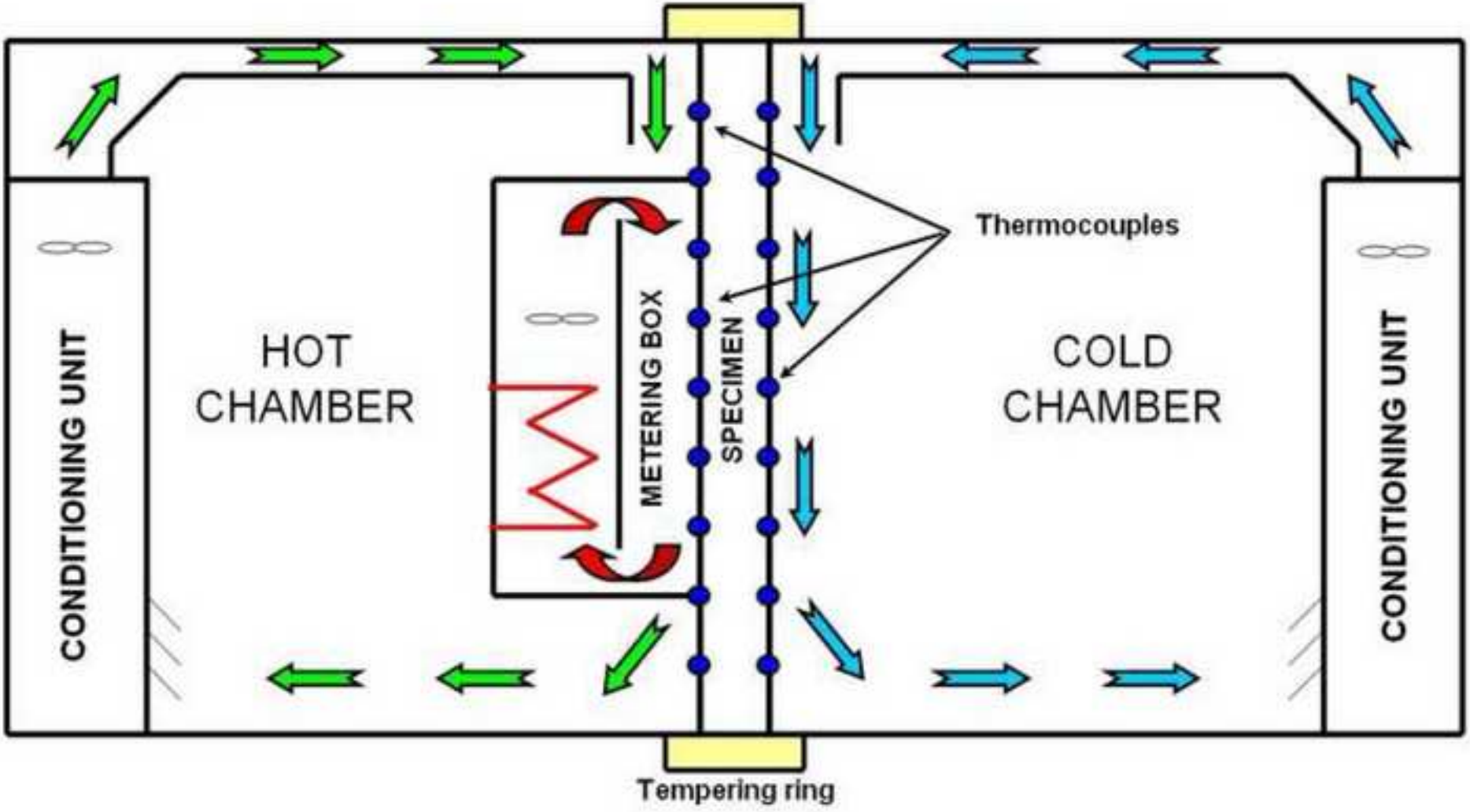
CONDITIONING UNIT
HOT CHAMBER
METERING BOX
SPECIMEN
Thermocouples
COLD CHAMBER
CONDITIONING UNIT
Tempering ring

Figure3

Figure4

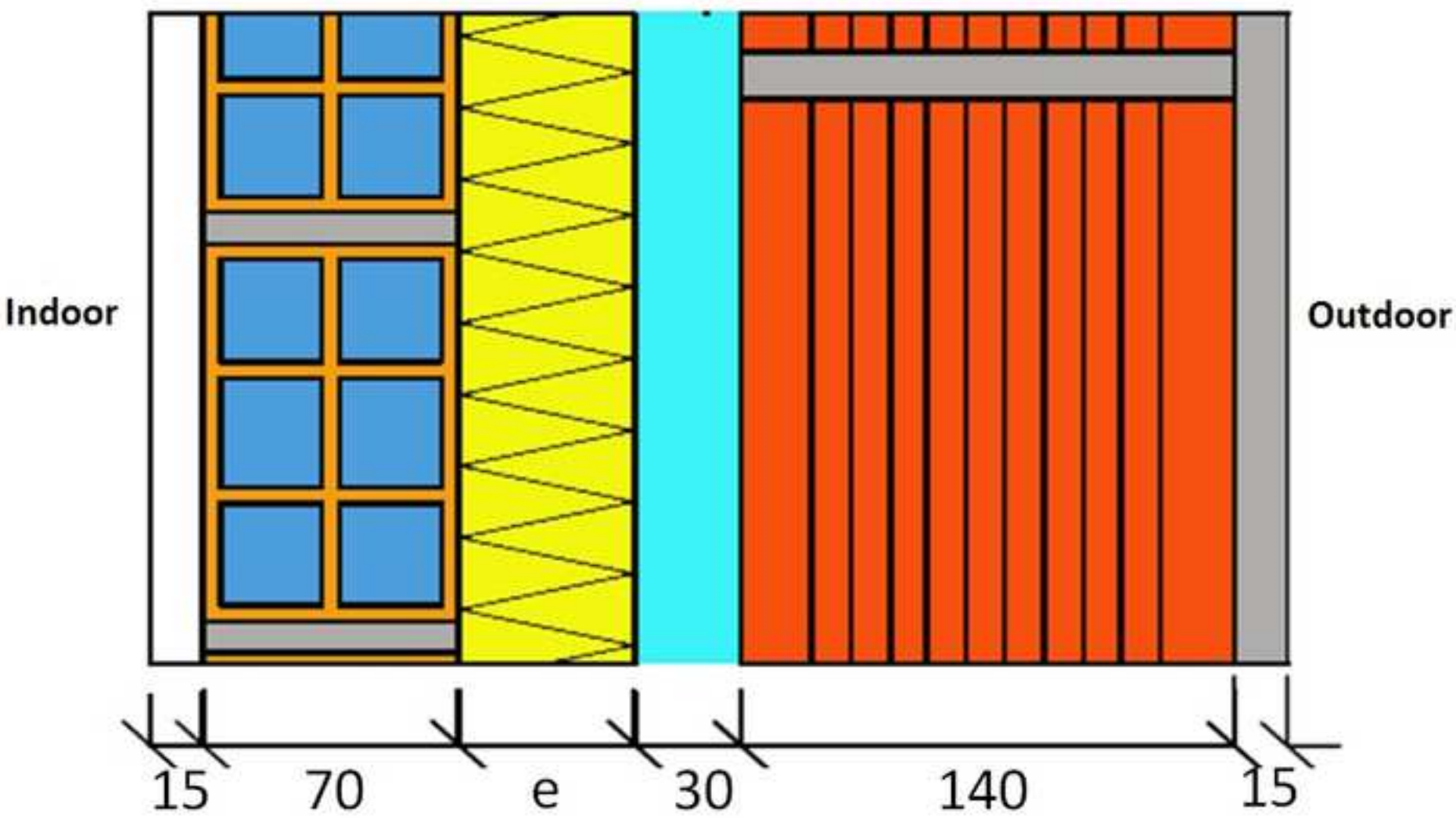

Figure5

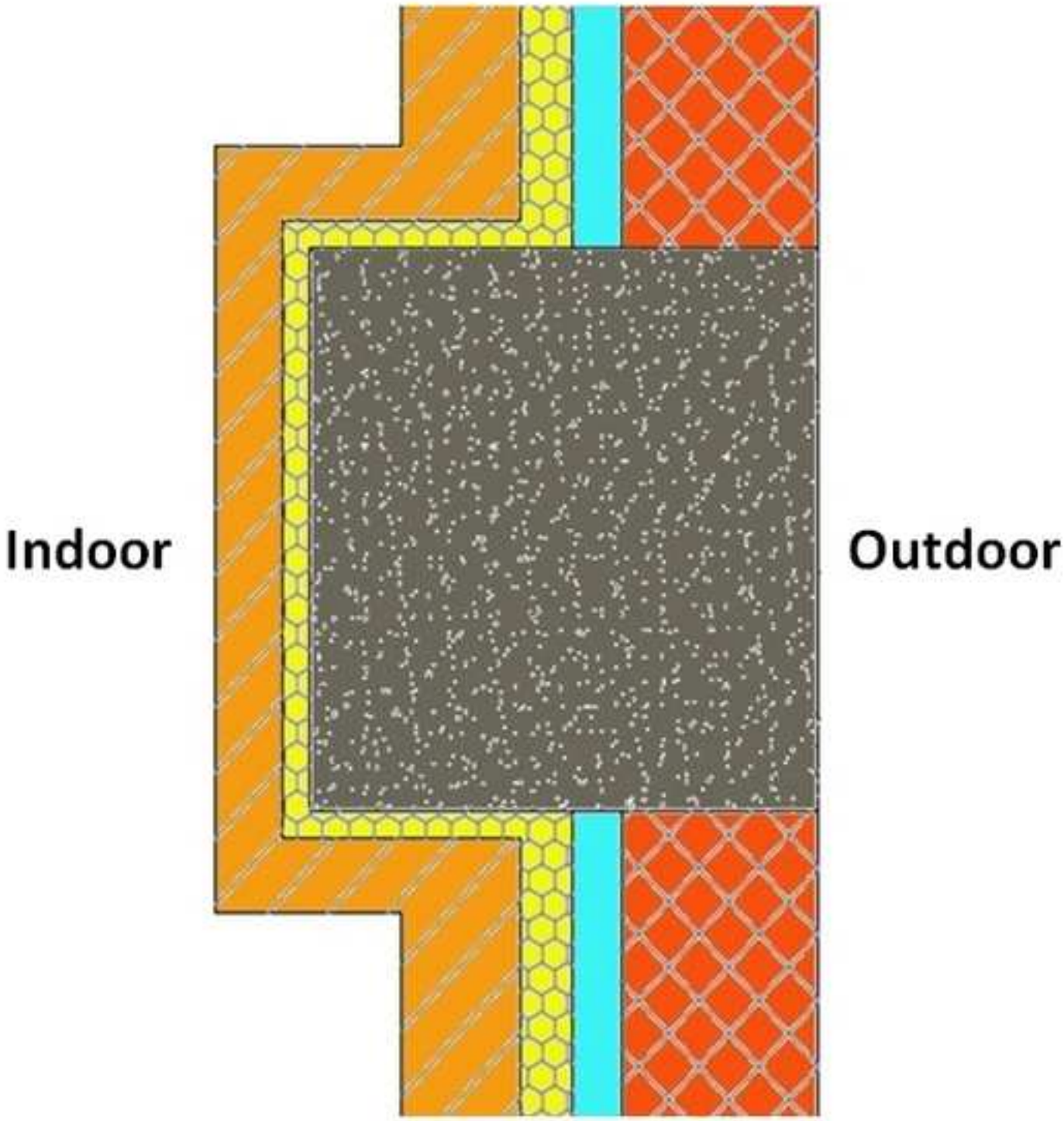

Figure6

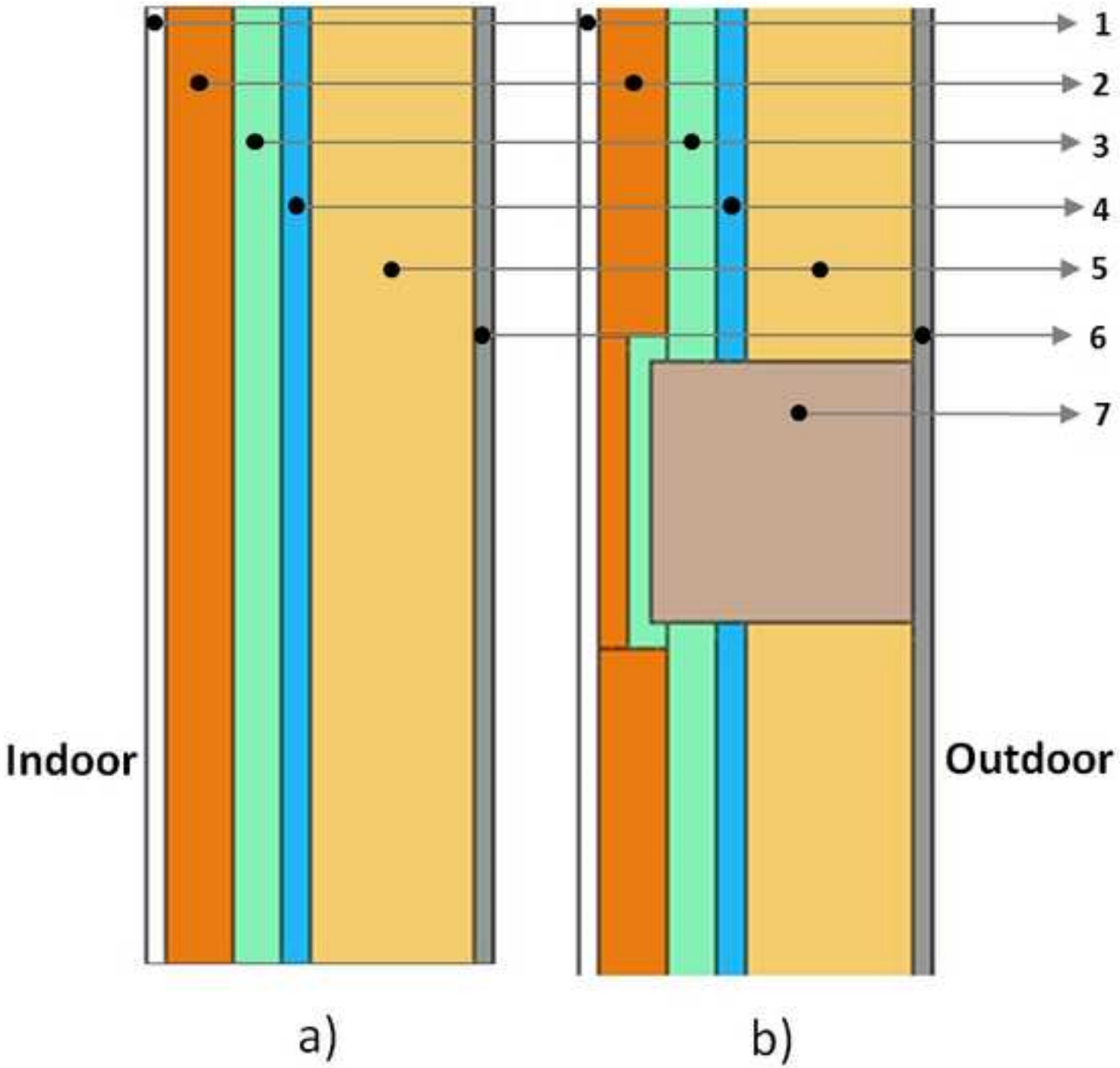

Figure7

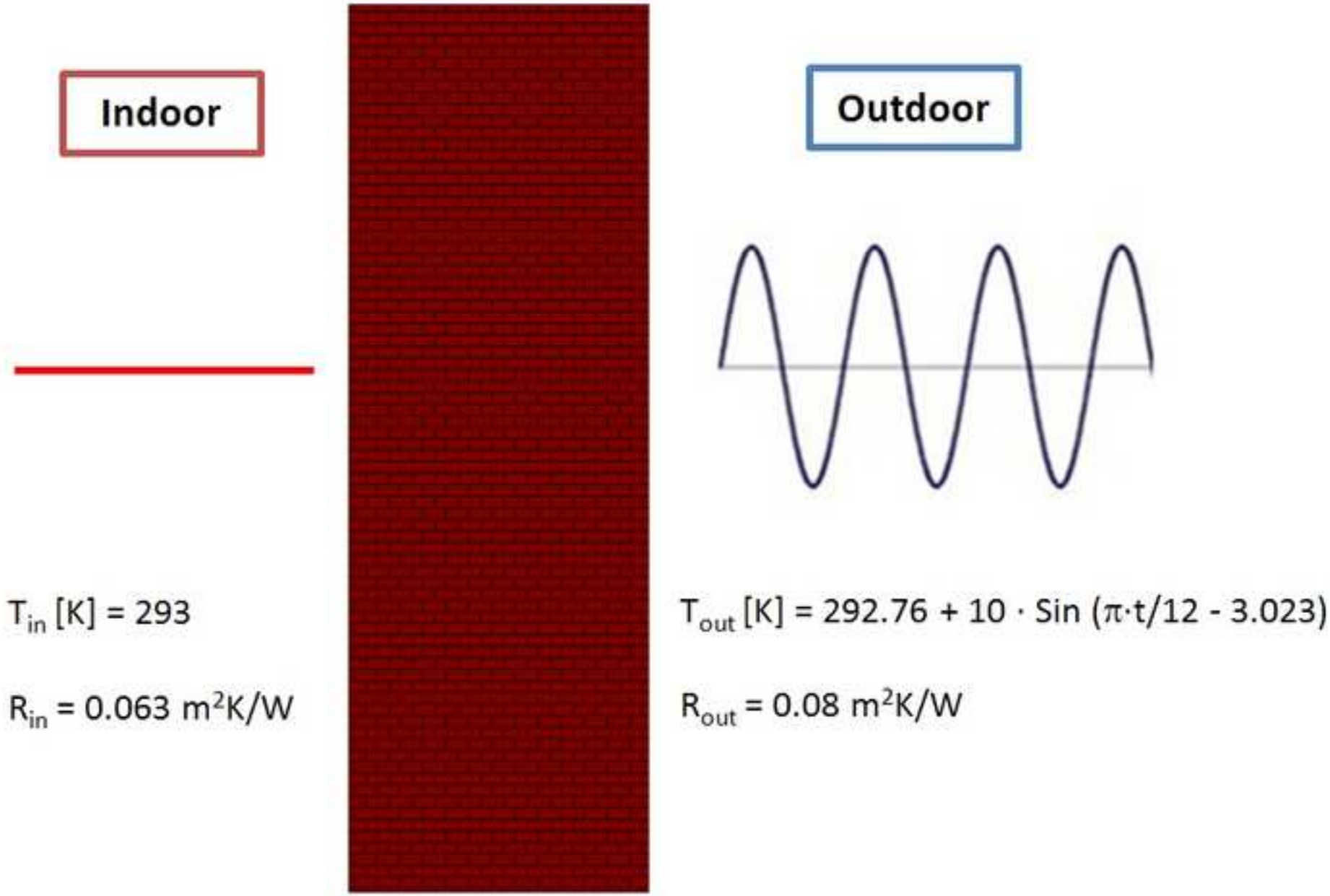
Indoor
Outdoor
T_{in} [K] = 293
R_{in} = 0.063 m^2K/W
T_{out} [K] = 292.76 + 10 · Sin (π·t/12 - 3.023)
R_{out} = 0.08 m^2K/W

Figure8

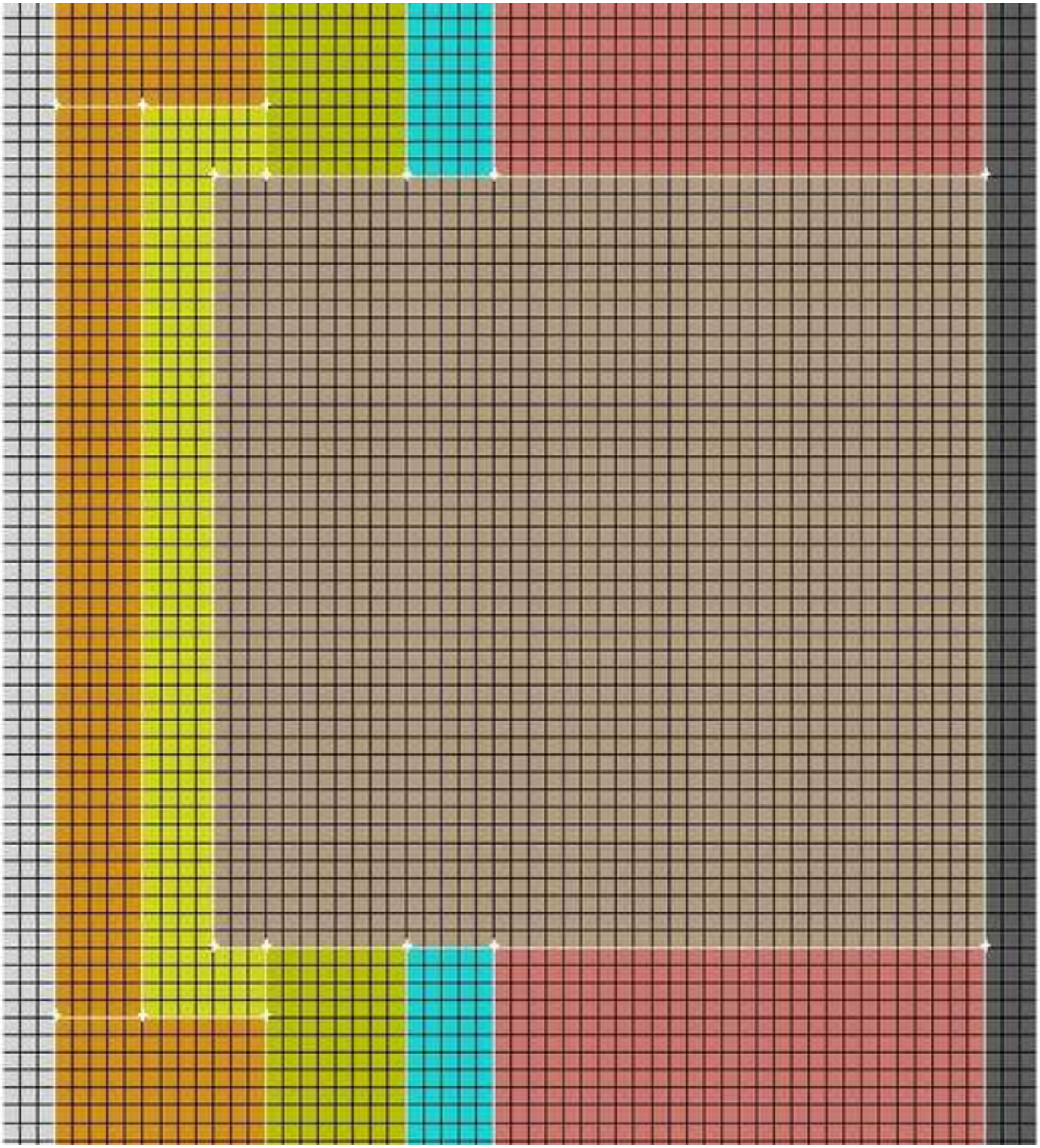

Figure9

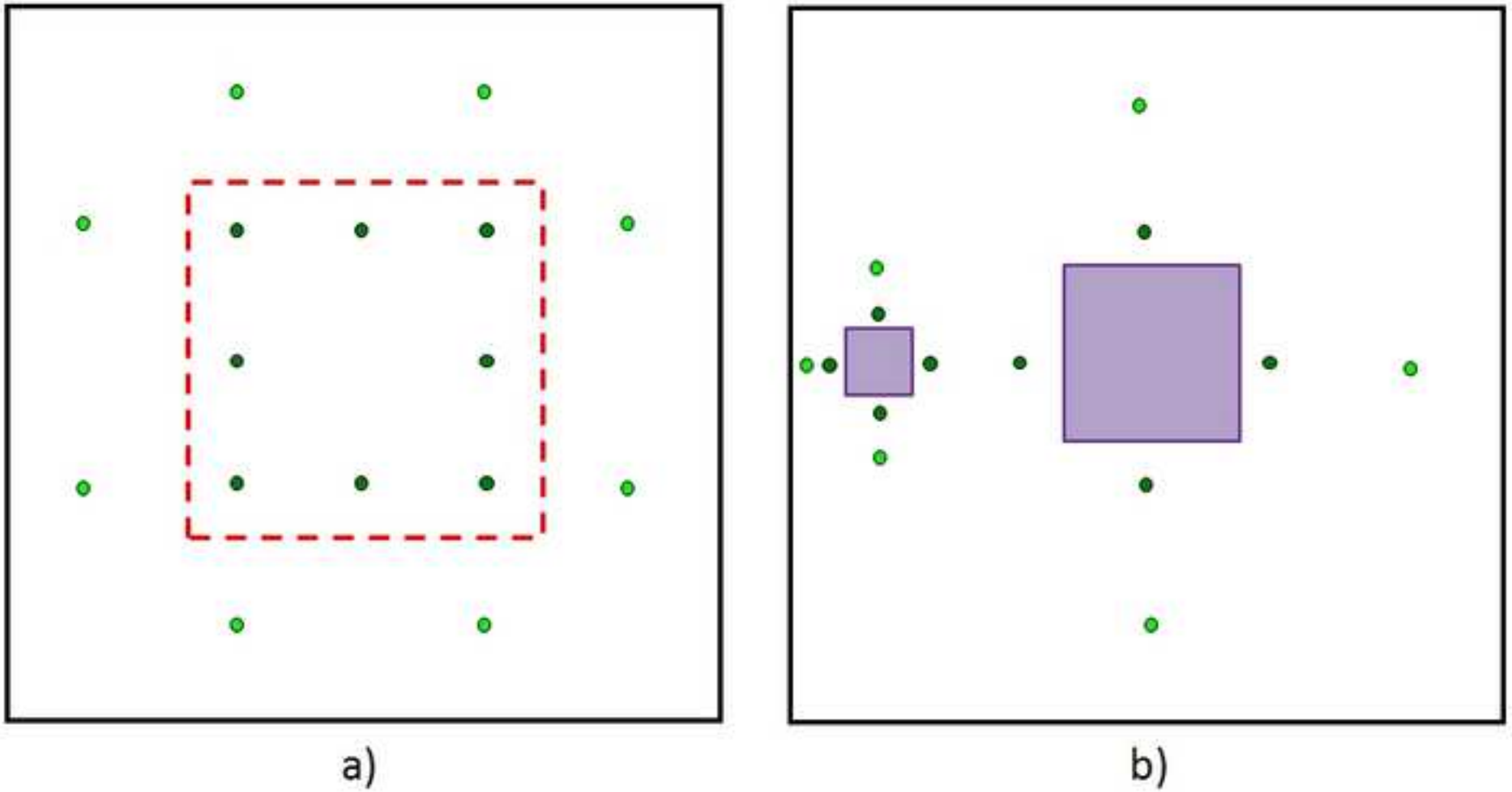

Figure10

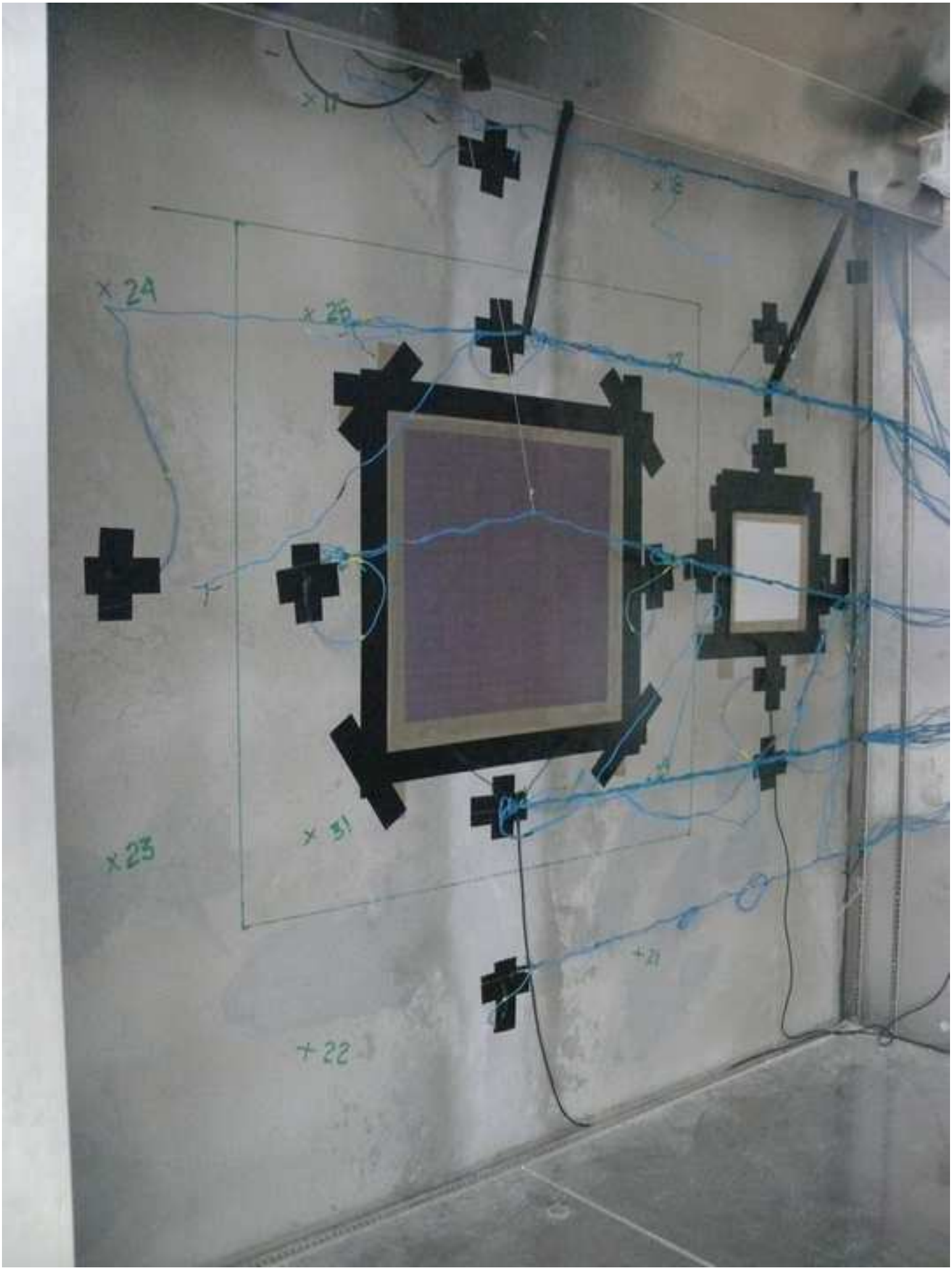

Figure11

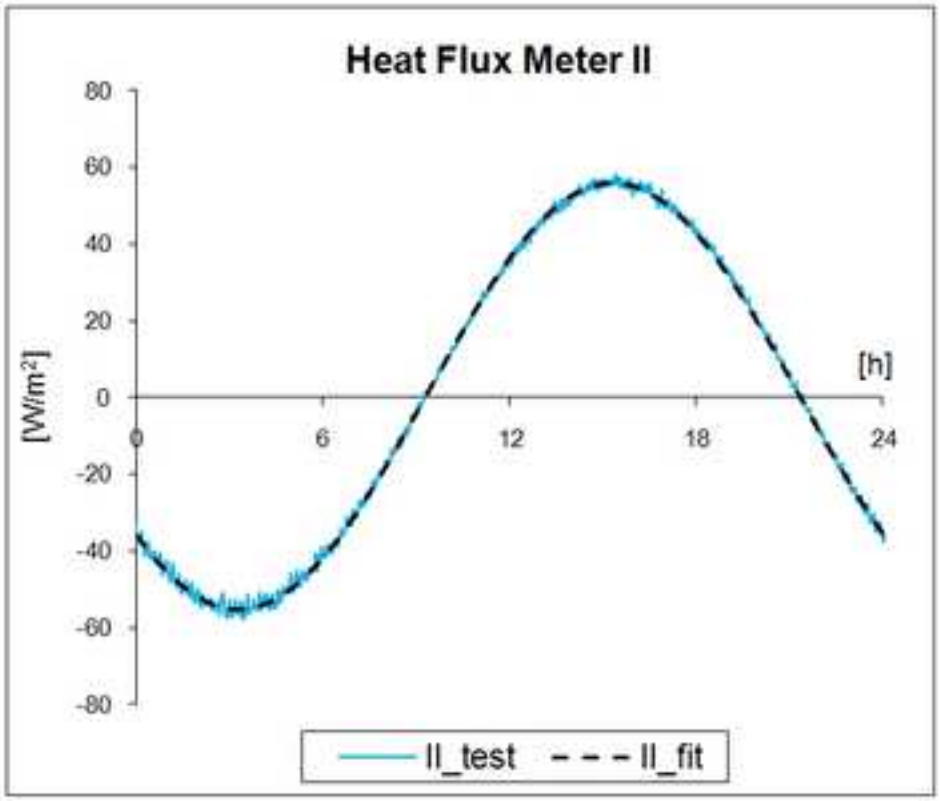
Heat Flux Meter II
80
60
40
20
0
-20
-40
-60
-80
[W/m²]
[h]
0
6
12
18
24
II_test
II_fit

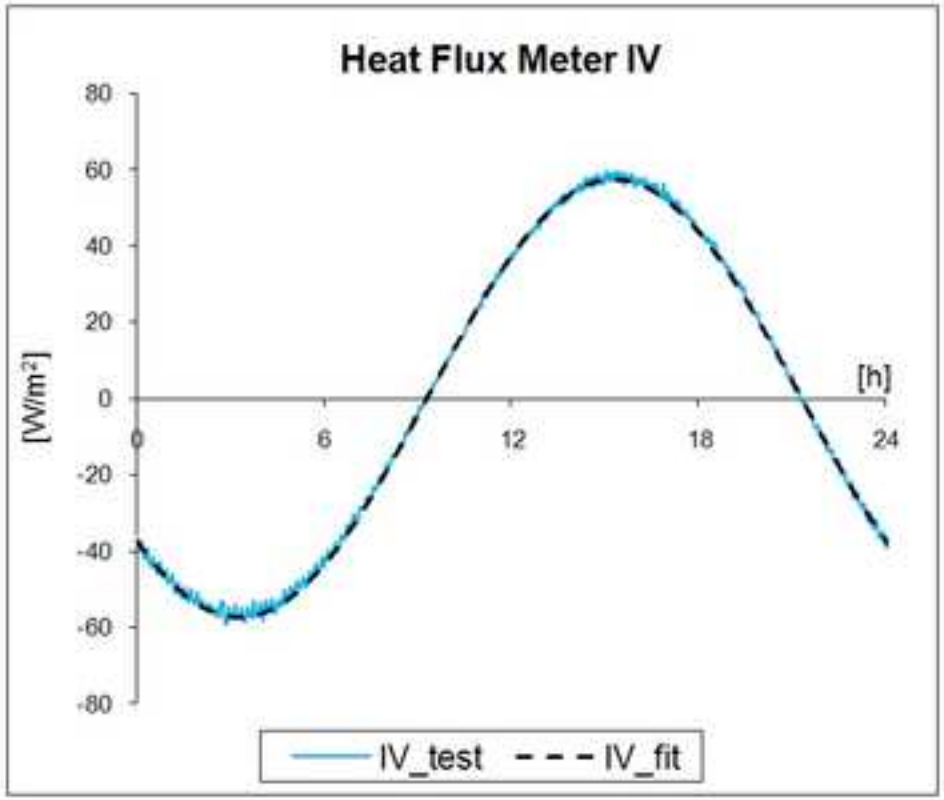
Heat Flux Meter IV
80
60
40
20
0
-20
-40
-60
-80
[W/m²]
[h]
0
6
12
18
24
IV_test
IV_fit

Figure12

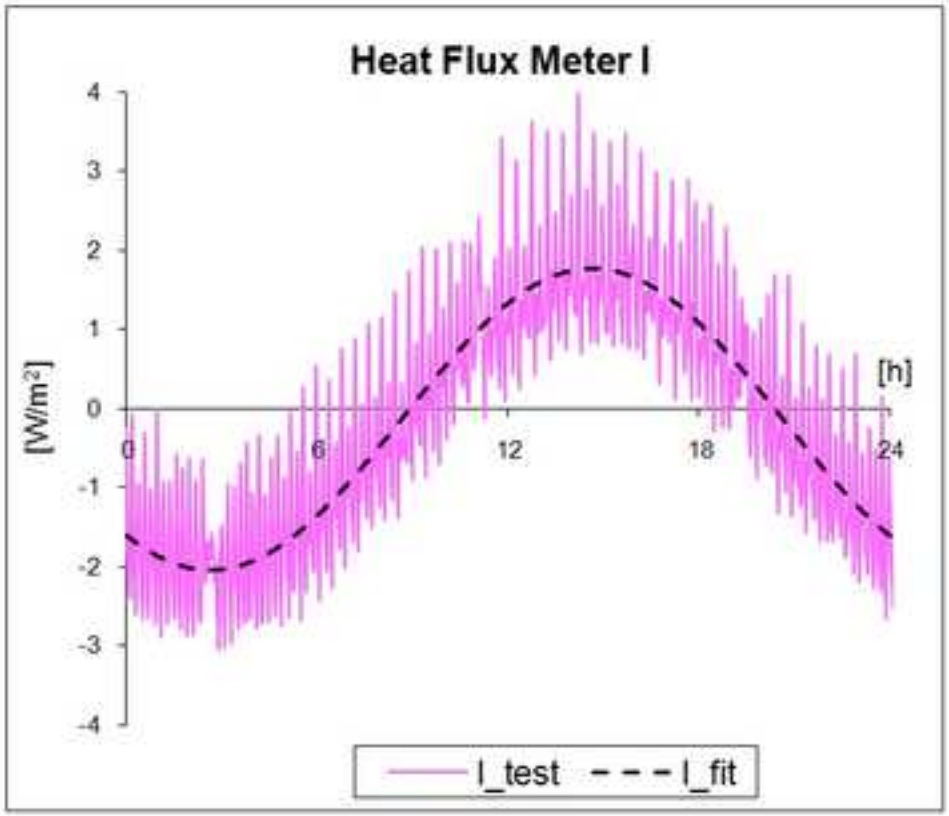
Heat Flux Meter I
[W/m²]
[h]
4
3
2
1
0
-1
-2
-3
-4
0
6
12
18
24
I_test
I_fit

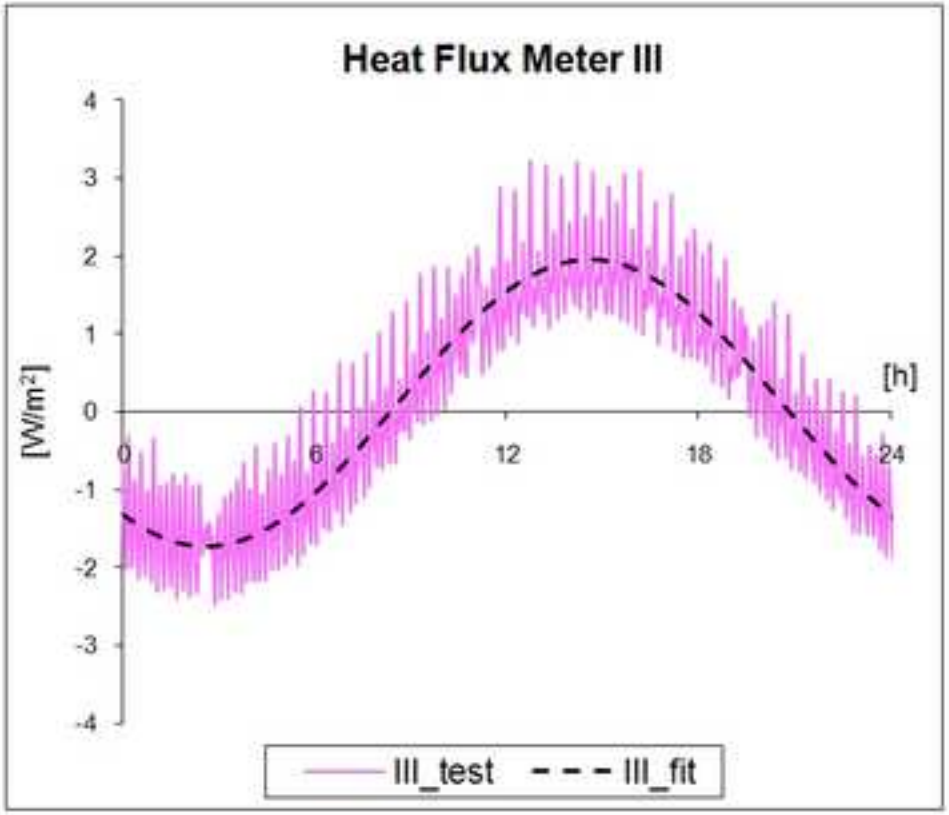
Heat Flux Meter III
[W/m²]
[h]
4
3
2
1
0
-1
-2
-3
-4
0
6
12
18
24
III_test
III_fit

Figure13

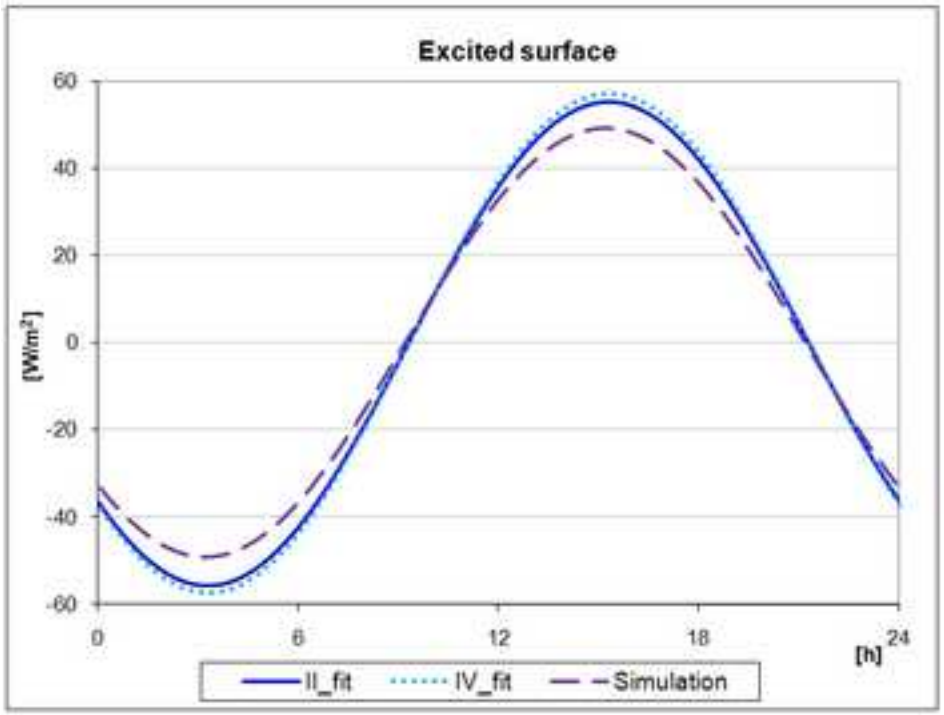
Excited surface
60
40
20
0
-20
-40
-60
[W/m²]
0
6
12
18
24
[h]
II_fit
IV_fit
Simulation

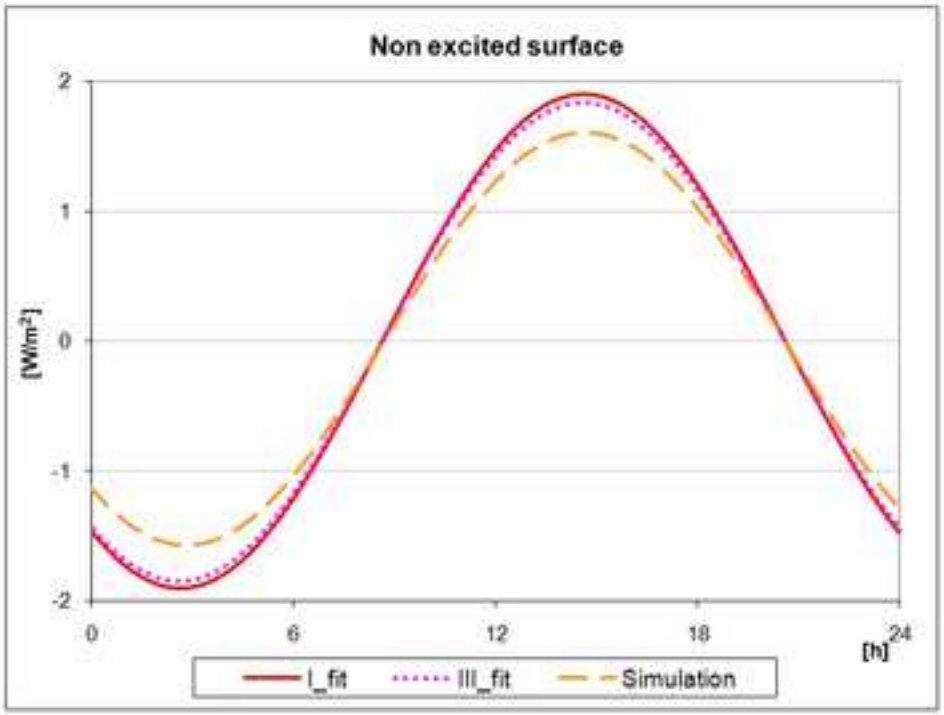
Non excited surface
2
1
0
-1
-2
[W/m²]
0
6
12
18
24
[h]
I_fit
III_fit
Simulation

Figure14

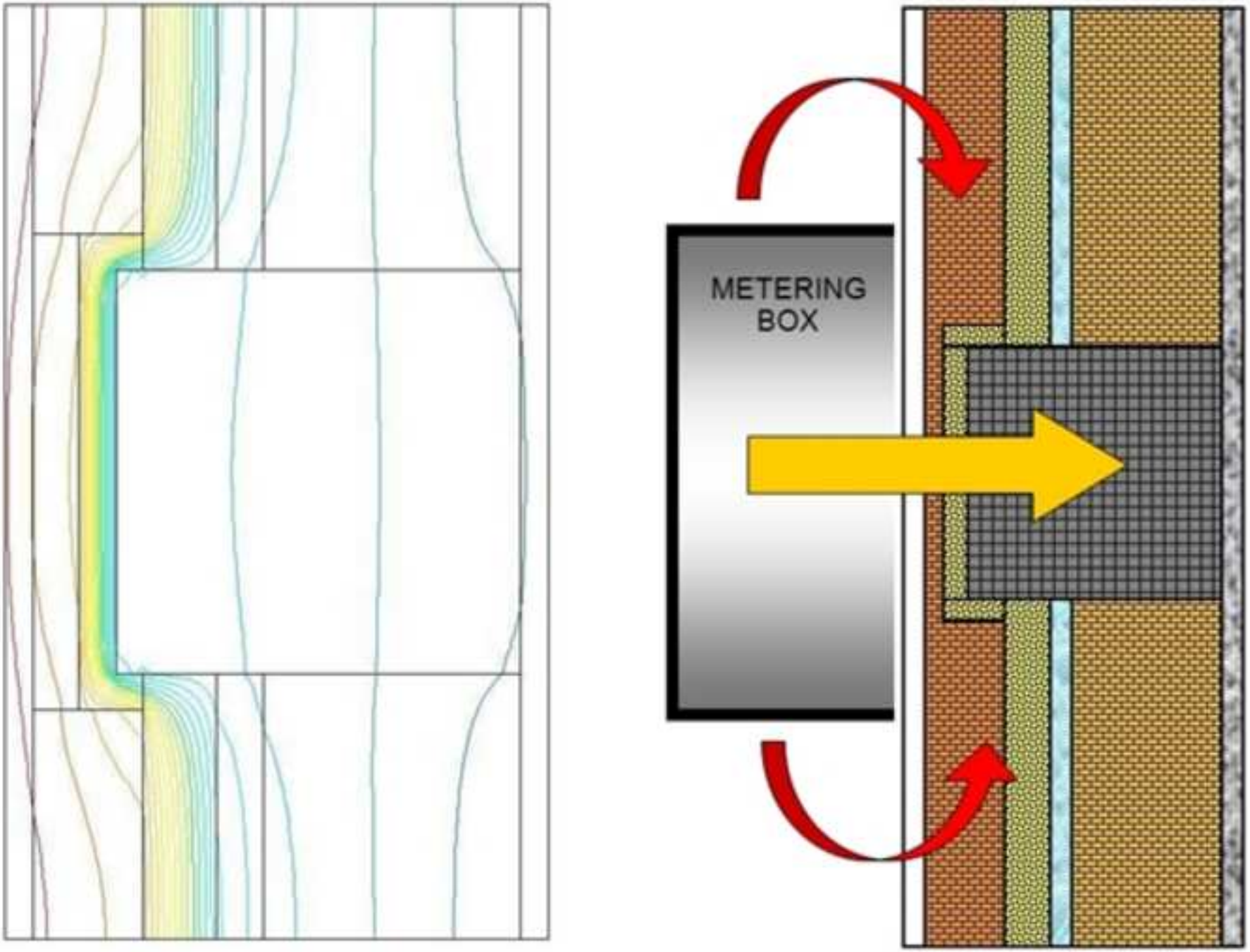

Figure15

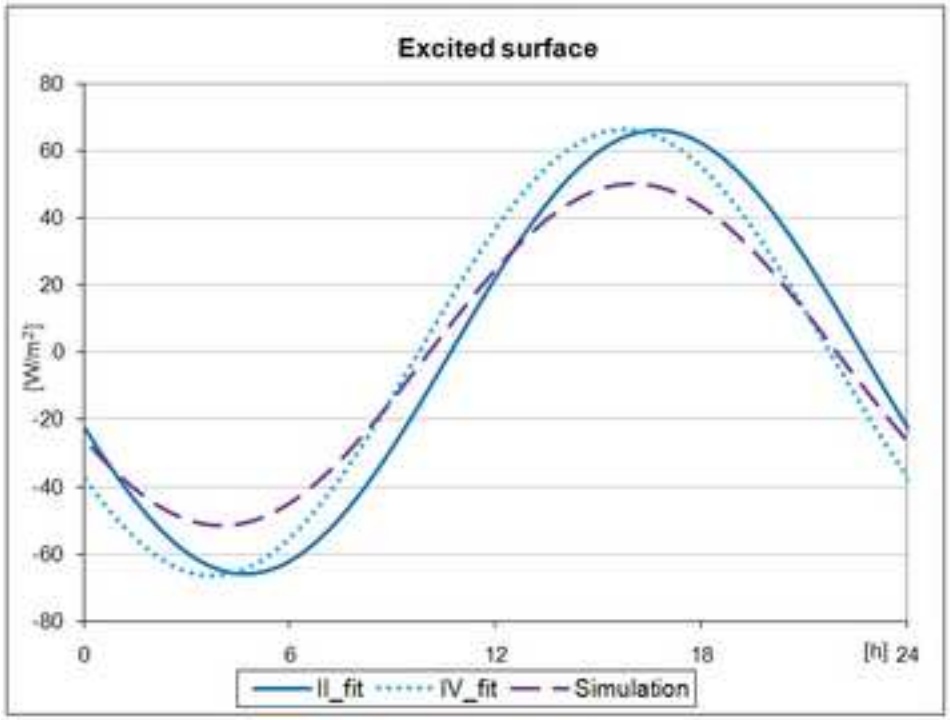
Excited surface
80
60
40
20
0
-20
-40
-60
-80
[W/m²]
0
6
12
18
[h] 24
II_fit
IV_fit
Simulation

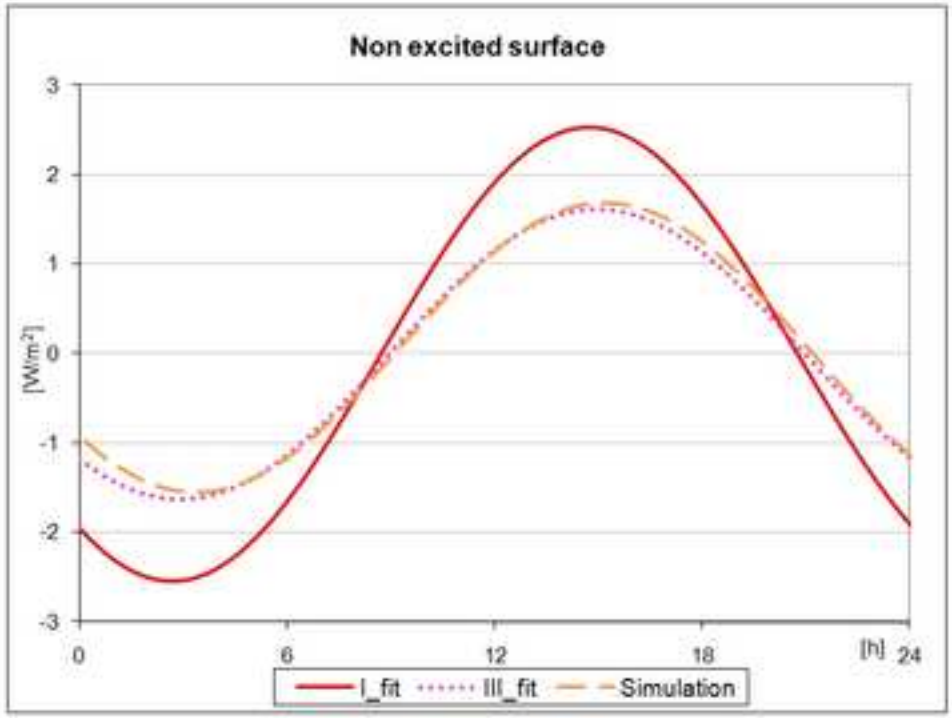
Non excited surface
3
2
1
0
-1
-2
-3
[W/m²]
0
6
12
18
[h] 24
I_fit
III_fit
Simulation

Figure16

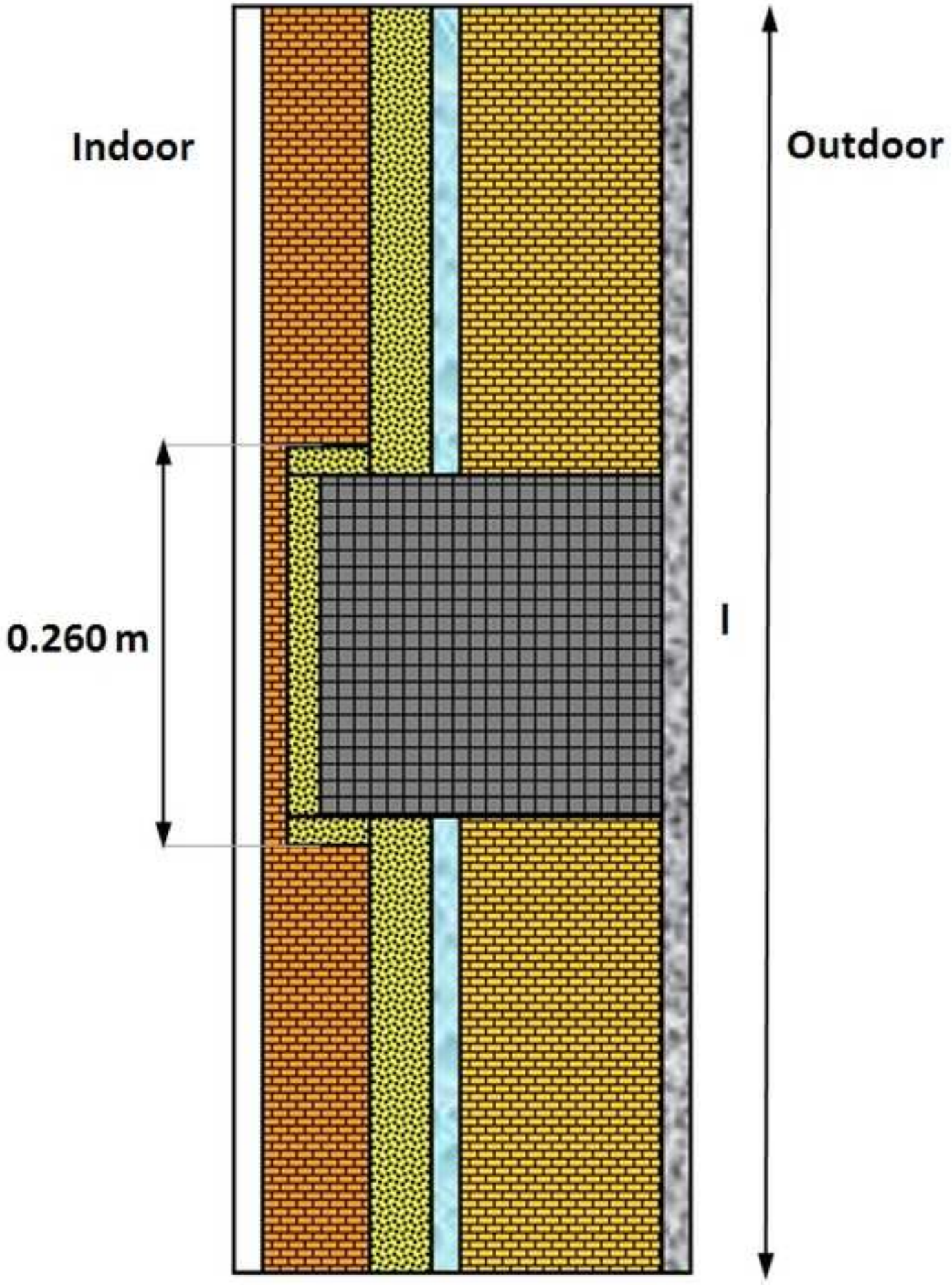

Figure17

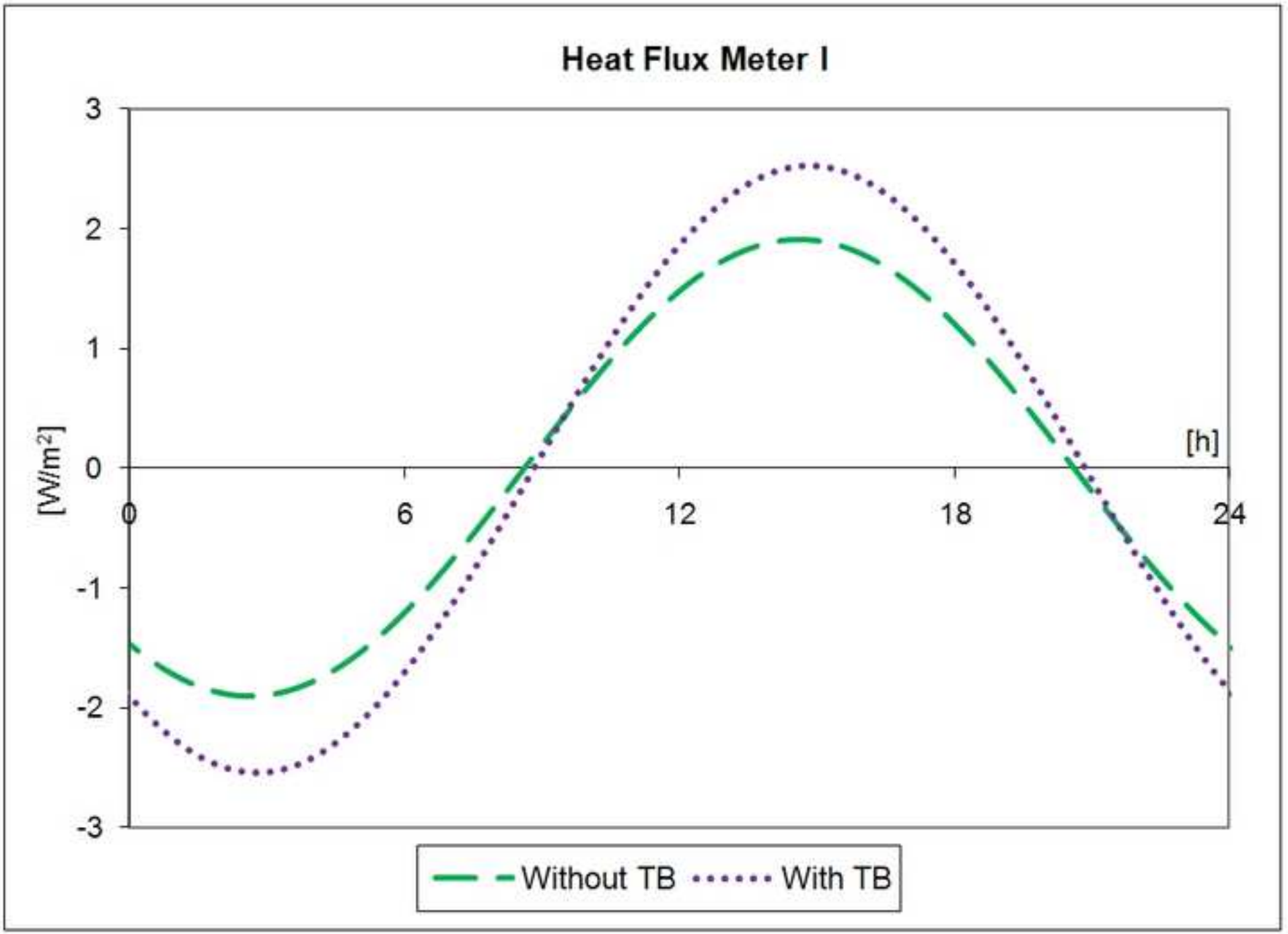

Figure18

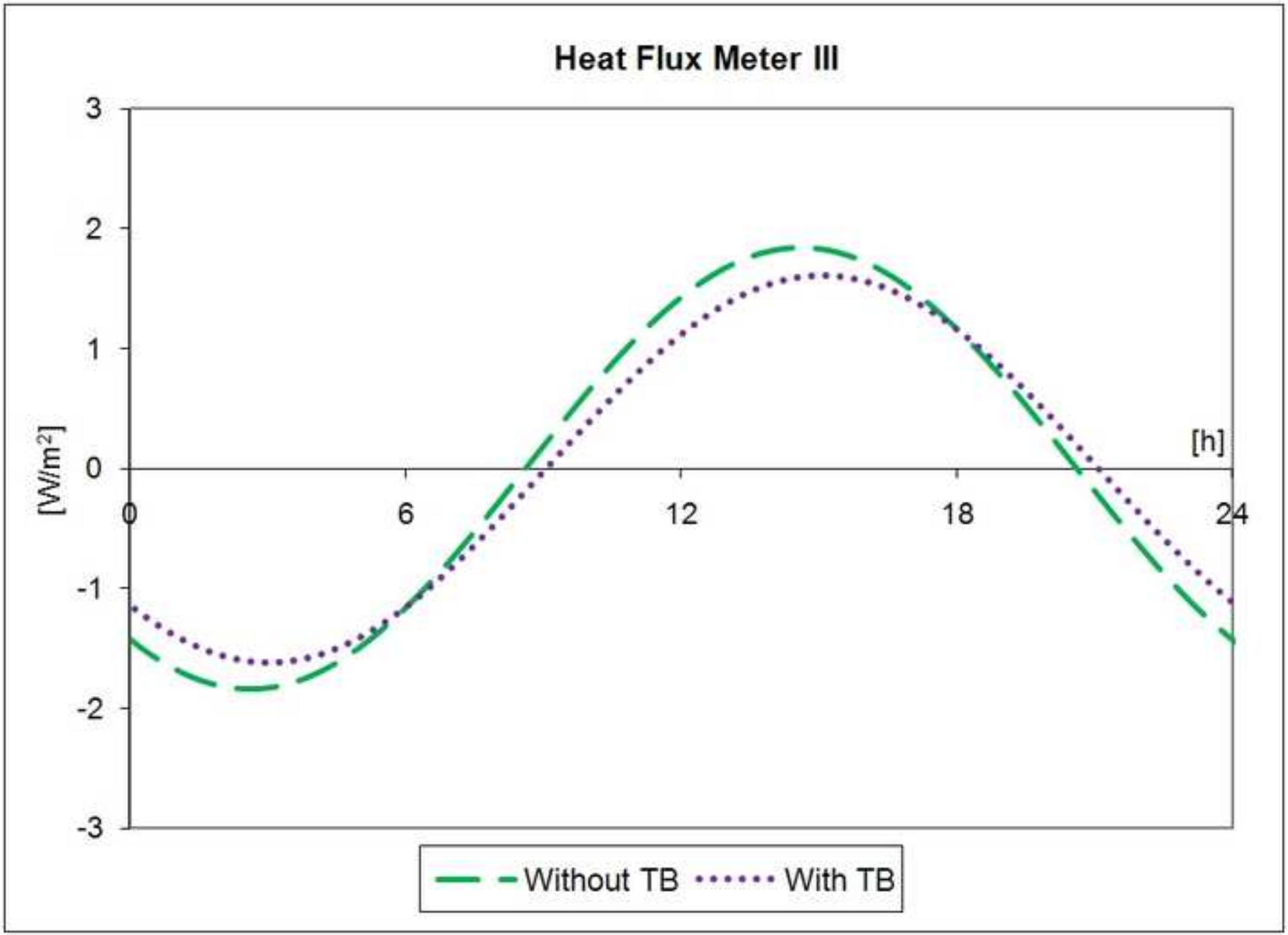
Heat Flux Meter III
3
2
1
0
-1
-2
-3
[W/m²]
[h]
0
6
12
18
24
Without TB
With TB

***Highlights**

- A pillar thermal bridge is tested in a hot box facility.
- Then it is compared with the homogeneous constructive solution.
- The effect in phase lag and amplitude is analyzed by test and simulation.
- Similar inertia and bigger amplitude is achieved in the thermal bridge.
- There is a need of redefining the cut-off planes for dynamic characterization.